

# Safe Task Planning for Language-Instructed Multi-Robot Systems using Conformal Prediction

Jun Wang, Guocheng He, and Yiannis Kantaros

**Abstract**—This paper addresses task planning problems for language-instructed robot teams. Tasks are expressed in natural language (NL), requiring the robots to apply their capabilities (e.g., mobility, manipulation, and sensing) at various locations and semantic objects. Several recent works have addressed similar planning problems by leveraging pre-trained Large Language Models (LLMs) to design effective multi-robot plans. However, these approaches lack mission performance and safety guarantees. To address this challenge, we introduce a new decentralized LLM-based planner that is capable of achieving high mission success rates. This is accomplished by leveraging conformal prediction (CP), a distribution-free uncertainty quantification tool in black-box models. CP allows the proposed multi-robot planner to reason about its inherent uncertainty in a decentralized fashion, enabling robots to make individual decisions when they are sufficiently certain and seek help otherwise. We show, both theoretically and empirically, that the proposed planner can achieve user-specified task success rates while minimizing the overall number of help requests. We demonstrate the performance of our approach on multi-robot home service applications. We also show through comparative experiments, that our method outperforms recent centralized and decentralized multi-robot LLM-based planners in terms of its ability to design correct plans. The advantage of our algorithm over baselines becomes more pronounced with increasing mission complexity and robot team size.

## I. INTRODUCTION

In recent years, the field of robotics has witnessed a paradigm shift towards the deployment of multiple robots collaborating to accomplish complex missions where effective coordination becomes paramount [1]–[3]. To this end, several multi-robot task planning algorithms have been proposed. These planners, given a high-level mission, can allocate tasks to robots and then design individual sequences of high-level actions to accomplish the assigned tasks [4]–[8]. Execution of these action plans is achieved using low-level motion planners and controllers [9]–[11]. A comprehensive survey on task and motion planning can be found in [12], [13]. Despite these notable achievements in robot planning, a recurrent limitation in these techniques is the substantial user expertise often required for mission specification using e.g., formal languages [14] or reward functions [15].

Motivated by the remarkable generalization abilities of pre-trained Large Language Models (LLMs) across diverse task domains [16]–[18], utilizing LLMs for task planning has been increasingly gaining attention. LLMs facilitate task definition in a user-friendly manner using natural language (NL),

J. Wang, G. He and Y. Kantaros are with the Department of Electrical and Systems Engineering, Washington University in St Louis. {junw, guocheng, ioannisk}@wustl.edu

This work was supported in part by the NSF award CNS #2231257 and the ARL grant DCIST CRA W911NF-17-2-0181.

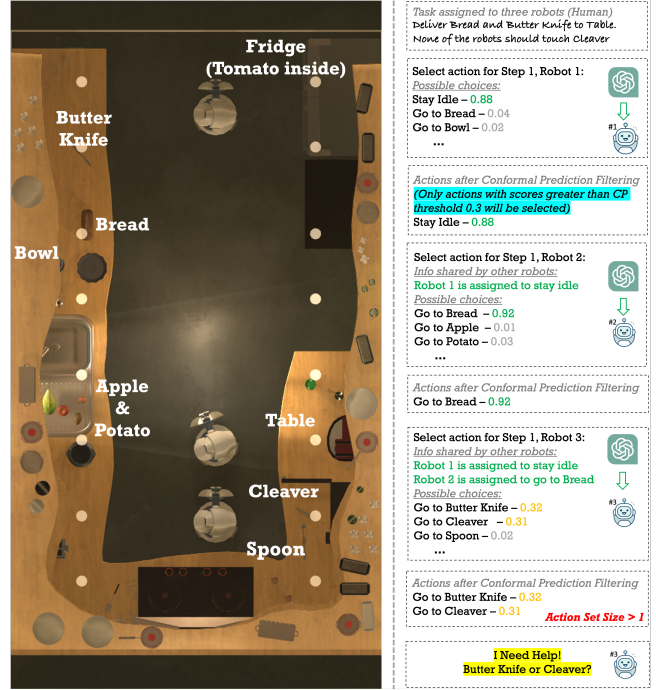


Fig. 1: We propose a decentralized planner for language-instructed multi-robot systems being capable of achieving user-specified mission success rates. The robots are delegated to pre-trained Large Language Models (LLMs), enabling them to select actions while coordinating in a conversational manner. Our LLM-based planner reasons about its inherent uncertainty, using conformal prediction, in a decentralized fashion. This capability allows the planner to determine when and which robot is uncertain about correctness of its next action. In cases of high uncertainty, the respective robots seek assistance.

empowering robots to design plans through conversational interactions. Early efforts primarily focused on single-robot task planning problems [18]–[34] while recent extensions to multi-robot systems are presented in [35]–[43]. These multi-robot planners either delegate each robot to an LLM for decentralized plan construction, use LLMs as centralized planners, or explore hybrid multi-agent communication architectures. Additionally, mechanisms to detect conflicts, such as collisions in the plans, and provide feedback to the LLMs for plan revision have been integrated into these frameworks. A detailed survey can be found in [44], [45]. A major challenge with current LLM-based planners is that they typically lack mission performance and safety guarantees while they often hallucinate, i.e., they confidently generate incorrect and possibly unsafe outputs.

This paper focuses on enhancing the reliability of LLM-based multi-robot planners. We consider teams of robots

possessing various skills such as mobility, manipulation, and sensing and tasked with high-level mission expressed using NL. Mission accomplishment requires the robots to apply their skills to various known semantic objects that exist in the environment. Our overarching goal is to design language-based planners capable of computing multi-robot plans (defined as sequences of robot actions) to achieve desired mission success rates. This necessitates developing planners that can reason about their inherent uncertainty, enabling robots to make decisions when sufficiently certain and seek help otherwise.

To address this problem, we propose a new decentralized LLM-based planner tightly coupled with conformal prediction (CP), a distribution-free uncertainty quantification tool for black-box models [46]–[48]; see also Fig. 1. In our framework, at each time step, the robots sequentially select actions while considering actions chosen by other robots. Each robot is delegated to a pre-trained LLM agent that is responsible for decision making. This coordinate-descent approach enables the decentralized construction of robot plans. To choose an action for a robot, we present the action selection problem to the corresponding LLM agent as a sequence of multiple-choice question-answering (MCQA) scenarios [31], [49]. Here, the ‘question’ corresponds to the textual task description and the history of past decisions, while the set of available ‘choices’ represents the skills that the selected robot can apply. The MCQA framework ensures that, unlike in other multi-robot planners, the LLM only chooses from valid choices, mitigating (partially) the risk of hallucination where invalid plans with nonsensical actions may be generated. Instead of simply selecting the action with the highest logit score, we employ CP to quantify the uncertainty of the employed LLM. This is crucial as LLMs tend to confidently generate incorrect outputs [49]. We show that CP can be used to design individual prediction sets for each robot given actions selected by other robots. This allows the LLM-based planner to determine when and, for which robot, it is uncertain about its predictions. In cases of high uncertainty, indicated by non-singleton prediction sets, the respective robots seek assistance from their robot teammates and/or human operators.

We provide comparisons showing that our planner outperforms related centralized and decentralized multi-robot planners in terms of its ability to design correct plans, even when the CP-based help-request module is omitted from our setup. This performance gap becomes more evident as the robot team size and the mission complexity increase. We contribute this trend to the MCQA-based framework as it attempts to prevent LLM hallucinations. In our comparisons, we also discuss trade-offs between token-efficiency and planning performance.

**Related Works:** As discussed earlier, several planners for language-driven robot teams have been proposed recently which, unlike the proposed method, lack performance guarantees. The closest works to ours are [49]–[51], as they apply CP for uncertainty alignment of LLMs. In [50], CP is applied to next-token prediction in MCQA tasks while [49], [51]

build upon that approach to address more general NL tasks with desired success rates. Notably, [49] is the first to demonstrate how CP can determine when a robot needs help from a user to efficiently resolve task ambiguities. These works, however, focus on single-robot planning problems. We remark that [49] can be applied straightforwardly to the multi-robot settings considered in this paper by simply treating the multi-robot system as a single-robot system that can perform multiple actions simultaneously. However, we show that such a centralized framework is both computationally expensive and token inefficient, resulting in prohibitive increases in API costs. Consequently, this limits its applicability to multi-robot and long-horizon missions. To the contrary, our approach is more token-efficient and scalable to multi-robot settings as it can construct, in a decentralized fashion, multi-robot plans and prediction sets. Moreover, adopting this centralized framework would yield multi-robot prediction sets, unlike the individual prediction sets constructed in this work. This could introduce additional challenges in determining which robot needs user assistance due to uncertainty about the correctness of its actions. We note that several uncertainty quantification and calibration methods for LLMs have been proposed recently that associate uncertainty with point-valued outputs [52]–[54]. Unlike these methods, CP generates prediction sets containing the ground truth output with user-specified probability providing coverage guarantees for the underlying model. CP has also been applied recently for various robotics tasks, such as perception [55]–[57], motion prediction [58]–[60], and decision making [61]; a comprehensive review of CP applications and implementations can be found in [62]. To the best of our knowledge, this paper proposes the first application of CP for language-based multi-robot planning, especially, in decentralized settings.

**Contribution:** The contribution of the paper can be summarized as follows. **(i)** We propose the first *decentralized* planner for language-instructed multi-robot systems that can achieve *user-specified task success rates*. **(ii)** We show how CP can be applied to construct multi-robot prediction sets in a decentralized fashion. **(iii)** We provide extensive comparative experiments demonstrating that the proposed planner outperforms related centralized/decentralized language-based planners in terms of planning performance.

## II. PROBLEM FORMULATION

**Robot Team:** Consider a team of  $N \geq 1$  mobile robots. Each robot is governed by the following dynamics:  $\mathbf{p}_j(t+1) = \mathbf{f}_j(\mathbf{p}_j(t), \mathbf{u}_j(t))$ ,  $j \in \{1, 2, \dots, N\}$ , where  $\mathbf{p}_j(t) \in \mathbb{R}^m$  stands for the state (e.g., position and orientation) of robot  $j$ , and  $\mathbf{u}_j(t) \in \mathbb{R}^b$  denotes the control input at discrete time  $t$ . We assume that all robot states are known for all time instants  $t \geq 0$ . Each robot possesses  $A > 0$  skills collected in a set  $\mathcal{A} \in \{1, \dots, A\}$ . These skills  $a \in \mathcal{A}$  are represented textually (e.g., ‘take a picture’, ‘grab’, or ‘go to’). The application of skill  $a$  by robot  $j$  to an object/region at location  $\mathbf{x}$  at time  $t$  is represented as  $s_j(a, \mathbf{x}, t)$ . For simplicity, we assume homogeneity among the robots, meaning they all share the same skill set  $\mathcal{A}$  and can apply skill  $a$  at any

given location  $\mathbf{x}$  associated with an object/region; later we discuss how this assumption can be relaxed. With slight abuse of notation, when it is clear from the context, we denote  $s_j(a, \mathbf{x}, t)$  by  $s_j(t)$  for brevity. We also define the multi-robot action at time  $t$  as  $\mathbf{s}(t) = [s_1(t), \dots, s_N(t)]$ . The time step  $t$  is increased by one, once  $\mathbf{s}$  is completed/executed. Additionally, we assume that every robot has access to low-level controllers to execute the skills in  $\mathcal{A}$ . We assume perfect execution of these skills.

**Environment:** The robot team resides in an environment  $\Omega \subseteq \mathbb{R}^d$ ,  $d \in \{2, 3\}$ , with obstacle-free space  $\Omega_{\text{free}} \subseteq \Omega$ . We assume that  $\Omega_{\text{free}}$  contains  $M > 0$  semantic objects. Each object  $e$  is defined by its location  $\mathbf{x}_e$  and a semantic label  $o_e \in \mathcal{O}$ , where  $\mathcal{O}$  is a set encompassing all semantic labels recognizable by the robots (e.g., ‘bottle’, ‘chair’, ‘person’, etc). Using the action space  $\mathcal{A}$  and the available semantic objects, we can construct a set  $\mathcal{S}$  that collects all possible decisions  $s_j$  that a robot can make. Notice that since we consider homogeneous robots, the set  $\mathcal{S}$  is the same for all robots  $j$ . We assume that both the obstacle-free space and the locations/labels of all objects are a-priori known and static; in Section III, we discuss how this assumption can be relaxed.

**Mission Specification:** The team is assigned a high-level coordinated task  $\phi$ , expressed in natural language (NL), that is defined over the objects or regions of interest in  $\Omega_{\text{free}}$ ; see Figure 1. Note that  $\phi$  may comprise multiple sub-tasks that are not necessarily pre-assigned to specific robots. Thus, achieving  $\phi$  involves determining which actions  $a$  each robot  $j$  should apply, when, where, and in what order. Our goal is to design multi-robot mission plans that accomplish  $\phi$ , defined as  $\tau = \mathbf{s}(1), \mathbf{s}(2), \dots, \mathbf{s}(H)$ , for some horizon  $H > 0$ . We formalize this by considering a distribution  $\mathcal{D}$  over scenarios  $\xi_i = \{N_i, \mathcal{A}_i, \phi_i, H_i, \Omega_i\}$ , with corresponding ground truth plans  $\tau_i$ .<sup>1</sup> Recall that  $N_i, \mathcal{A}_i, \phi_i, H_i$ , and  $\Omega_i$  refer to the number of homogeneous robots, the robot skills, the language-based task, the mission horizon, and the semantic environment, respectively, associated with  $\xi_i$ . The horizon  $H_i$  essentially determines an upper bound on the number of steps  $t$  required to accomplish  $\phi_i$ . The subscript  $i$  is used to emphasize that these parameters can vary across scenarios. We assume that all scenarios  $\xi_i$  drawn from  $\mathcal{D}$  are feasible in the sense that  $H_i$  is large enough and all objects of interest are accessible to the robots. When it is clear from the context, we drop the dependence on  $i$ . Note that  $\mathcal{D}$  is unknown but we assume that we can sample i.i.d. scenarios from it. Our goal is to design language-based planners that generate correct plans  $\tau_i$  in at least  $(1 - \alpha) \cdot 100\%$  of scenarios  $\xi_i$  drawn from  $\mathcal{D}$ , for some user-specified  $\alpha \in [0, 1]$ .

**Problem Statement:** In this paper, our goal is to address the following problem:

*Problem 1:* Consider an unknown distribution  $\mathcal{D}$  over multi-robot scenarios  $\xi$ . Design a task planner generating plans  $\tau$  performing the missions correctly in at least  $(1 -$

<sup>1</sup>To account for heterogeneous robots, more complex distributions  $\mathcal{D}$  can be defined that generate action sets for each robot separately. The algorithm presented in Section III remains applicable. We abstain from this presentation for the sake of simplicity.

---

### Algorithm 1 Safe Language-based Multi-robot Planning

---

```

1: Input: Scenario  $\xi$ ; Coverage level  $\alpha$ ; Upper bound  $W$ 
2: Initialize an ordered set  $\mathcal{I}$ ;
3: Initialize prompt  $\ell_{\mathcal{I}(1)}(1)$  with empty history of actions
4: for  $t = 1$  to  $H$  do
5:   Initialize help counter  $w = 0$ 
6:    $\mathbf{s}(t) = [\emptyset, \dots, \emptyset]$ 
7:   for  $i \in \mathcal{I}$  do
8:     Next robot  $j = \mathcal{I}(i)$ 
9:     Compute  $\ell_j(t)$  using  $\ell_{j-1}(t)$ 
10:    Compute the prediction set  $\mathcal{C}(\ell_j(t))$  as in (9)
11:    if  $|\mathcal{C}(\ell_j(t))| > 1$  then
12:       $w = w + 1$ 
13:    if  $w > W$  then
14:      Obtain  $s_j(t)$  from human operator
15:    else
16:      Get new  $\mathcal{I}'$ , set  $\mathcal{I} = \mathcal{I}'$ , and go to line 6
17:    else
18:      Pick the (unique) decision  $s_j(t) \in \mathcal{C}(\ell_j(t))$ 
19:      Update  $\ell_j(t) = \ell_j(t) + s_j(t)$ 
20:      Send  $\ell_j(t)$  to robot  $\mathcal{I}(i+1)$ 
21:    Construct  $\mathbf{s}(t) = [s_1(t), \dots, s_N(t)]$ 
22:    Append  $\mathbf{s}(t)$  to the multi-robot plan  $\tau$ 

```

---

$\alpha) \cdot 100\%$  of scenarios drawn from  $\mathcal{D}$ , for a user-specified  $\alpha \in [0, 1]$ .

### III. SAFE PLANNING FOR LANGUAGE-INSTRUCTED ROBOT TEAMS

We propose a new mission planner that harnesses pre-trained LLMs to address Problem 1; see Alg. 1. In Section III-A, we present a centralized solution, building upon [49], which we show to be token inefficient. Motivated by this limitation, in Sections III-B-III-C, we propose a decentralized planner. The developed algorithm can reason about its inherent uncertainty, allowing the robots to make decisions when certain enough, and seek assistance otherwise.

#### A. A Centralized Planning Framework using LLMs

A potential solution to address Problem 1 is to directly apply the planning framework presented in [49] that is developed for single-robot task planning problems. The key idea in [49] is to present the task planning problem as a sequence of MCQA scenarios over time steps  $t \in \{1, \dots, H\}$ . In this setting, the question refers to the task  $\phi$  along with a textual description of any possible mission progress. The choices refer to decisions  $s_j(t) \in \mathcal{S}$  that the (single) robot  $j$  can make. Then, to pick the ‘best’ action at time  $t$ , the LLM is queried  $S = |\mathcal{S}|$  times. A more detailed description of the algorithm along with its mission success rate guarantees can be found in [49]. This setting can be applied in the considered multi-robot planning problem by simply treating the multi-robot system as a single robot that can apply  $N$  actions simultaneously. In this case, the number of choices/decisions  $\mathbf{s}(t)$  in the MCQA framework are  $S^N$ . Thus, the employed LLM has to be queried  $S^N$  times to pick a multi-robot

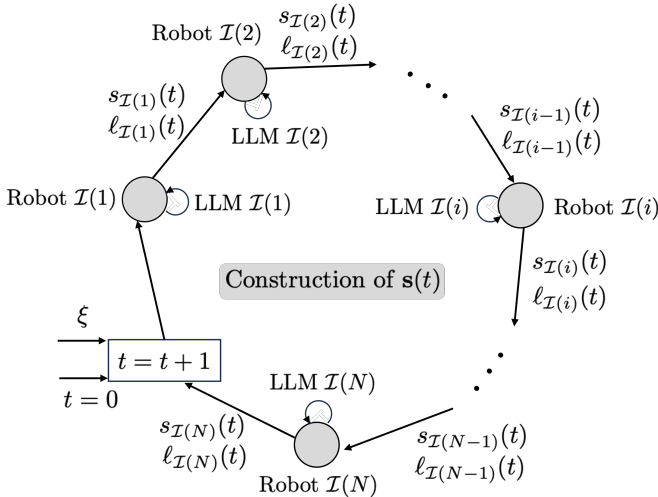


Fig. 2: Given a task scenario  $\xi$ , the robots select decisions at each time  $t$  sequentially as per an ordered set  $\mathcal{I}$  of robot indices. Each robot  $j = \mathcal{I}(i)$  (gray disk) is delegated to an LLM that generates a decision  $s_j(t)$  given textual context  $\ell_{\mathcal{I}(i-1)}(t)$  containing the task description and past robot decisions provided by the previous robot  $\mathcal{I}(i-1)$ . If the LLM for robot  $j$  is not certain enough about what the correct decision  $s_j(t)$  is, the robots seek assistance (not shown).

action at a single time step  $t$  which is impractical due to its high computational cost. Additionally, this can prohibitively increase the total API cost of using LLMs, especially, for long horizons  $H$  or large number  $N$  of robots; see Sec. V.

### B. Decentralized Multi-Robot Planning using LLMs

In this section, we propose a decentralized planning framework to address Problem 1 that is more efficient than the one presented in Section III-A and, therefore, it can scale to large robot teams and long mission horizons; see Remark 3.2. Our setup leverages coordinate-descent methods that have been used extensively to address multi-robot planning problems in a decentralized manner [63], [64]. The key idea is that, given a scenario  $\xi$  drawn from  $\mathcal{D}$ , the robots pick decisions at time  $t$  successively (as opposed to jointly in Section III-A). Each robot  $j$  is delegated to an LLM that picks a decision  $s_j(t)$ , using an MCQA setup, while incorporating decisions of past robot decisions. If the LLM for robot  $j$  is not certain enough about what the correct  $s_j(t)$  is, it seeks assistance from other robots and/or human operators. This process gives rise to the multi-robot decision  $\mathbf{s}(t)$  at time  $t$ . The above is repeated to construct  $\mathbf{s}(t+1), \dots, \mathbf{s}(H)$ . Next, we describe our proposed decentralized planning algorithm in more detail.

Consider a scenario  $\xi$  drawn from  $\mathcal{D}$  and an ordered set  $\mathcal{I}$ , initialized by a user, collecting robot indices  $j \in \{1, \dots, N\}$  so that each robot index appears exactly once; e.g.,  $\mathcal{I} = \{1, \dots, N\}$  [line 2, Alg. 1]. We denote the  $i$ -th element in  $\mathcal{I}$  by  $\mathcal{I}(i)$ . At each  $t \in \{1 \dots H\}$ , the robots pick actions sequentially as per  $\mathcal{I}$  [lines 3-22, Alg. 1]; see also Fig. 2. Specifically, robot  $j = \mathcal{I}(i)$  selects  $s_j(t)$  while considering, the NL task description as well as all decisions that have been made until  $t-1$  and all decisions made by the robots  $\mathcal{I}(1), \dots, \mathcal{I}(i-1)$  at time  $t$ . This information, denoted by  $\ell_j(t)$ , is described textually. Given the context  $\ell_j(t)$ , the LLM assigned to robot  $j$  generates  $s_j(t)$ . Hereafter, for

Action Space:	Environment Description		
(1, x): Go to object/container x	Location LA: tomato T1 and bottle B2 and potato P1		
(2, x): Pick up object x	Location LB: apple A1 and tomato T2		
(3, x): Put down object at location x	Location LC: Coke C1 in Fridge F (closed)		
(4, x): Open the door of container x	Location LD: apple A2 and Coke C2		
(5): Remain idle	Location LE: bottle B1 and potato P2		
Example Task		Response Structure	
There are three robots in the environment. Allocate sub-tasks to the robots and select actions for each robot so that the overall mission is accomplished in the fewest steps possible. Choose one action for each robot from the action space.		step1: R1:(1, F) R2:(1, A1) R3:(1, T1)	
Mission: Move C1 to LA or LD. Move A1 to LE. Move T1 or T2 to LD. Move P1 to LD. Move B1 to LB. Move B2 to LE. Move P2 to LB. Move C2 to LA. Robot 1 should not touch A1. Robot 2 should not open fridge doors		step4: R1:(3, LA) R2:(1, P1) R3:(1, B1)	
		step7: R1:(3, LE) R2:(2, P2) R3:(2, B1)	
		step8: R1:(5) R2:(2, A1) R3:(2, C1)	
		step9: R1:(2, B2) R2:(3, LD) R3:(3, LA)	
		R1:(2, C1) R2:(3, LD) R3:(3, LB)	

Fig. 3: Examples of parts (a) (only action space), (b), and (e) used to construct prompts in Section V.

simplicity of notation, we assume that  $\mathcal{I} = \{1, \dots, N\}$  so that  $\mathcal{I}(j) = j$ . We also assume that all agents share the same LLM model; this assumption is made only for ease of notation as it will be discussed later. Next, we first describe how  $\ell_j(t)$  is structured and then we discuss how  $s_j(t)$  is computed given  $\ell_j(t)$ .

**Prompt Construction:** The prompt  $\ell_j(t)$  consists of the following parts (see also Fig. 3): (a) *System description* that defines the action space  $\mathcal{A}$  that the robot can apply and rules that the LLM should always respect in its decision-making process. For instance, in our considered simulations, such rules explicitly determine that a robot cannot grasp an object located in a container (e.g., fridge) before opening it. We observed that explicitly specifying such constraints improved the quality of LLM plans. We also mention that decisions made by previous robots at the current time step  $t$  and the action that will be selected for current robot  $j$  at time  $t$  will be executed simultaneously (even though these decisions are designed sequentially). This aims to prevent any conflicts that may occur during plan execution.<sup>2</sup> We additionally require the length of the plan  $\tau$  to be less than some horizon  $H \geq 0$ . (b) *Environment description* that describes the locations of each semantic object of interest; (c) *Task description* that includes the task description  $\phi$ ; (d) *History of actions* that includes the sequence of decisions made by all robots up to time  $t-1$  and for all robots  $1, \dots, j-1$  up to time  $t$ . (e) *Response structure* describing the desired structure of the LLM output for an example task. (f) *Current time step and robot index* describing the current time step  $t$  and the index  $j$  to the robot that is now responsible for picking an action.

**Plan Design & Execution:** Assume that at time  $t$ , it is robot's  $j$  turn to select  $s_j(t)$  as per the order captured in  $\mathcal{I}$ . First, robot  $j$  constructs  $\ell_j(t)$  using the prompt  $\ell_{j-1}(t)$  that the previous robot  $j-1$  constructed (or  $\ell_N(t-1)$ , if  $j=1$ )

<sup>2</sup>For instance, consider the case where at time  $t$ , robot  $j-1$  has made the decision to open the fridge. Then, robot  $j$  at time  $t$  should not make a decision under the (incorrect) assumption that the fridge has already been opened at time  $t$ . This instruction attempts to eliminate such invalid plans. Conflicts in the plans can also be detected and resolved by using LLMs as in [40]. This, however, is out of the scope of this work.

[line 8-9, Alg. 1]. Parts (a)-(c) in  $\ell_j(t)$  are the same for all  $j$  and  $t \geq 1$  (since the environment is assumed static and known; see Rem. 3.1); part (d) includes the history of actions and can be found in part (d) of  $\ell_{j-1}(t)$ ; part (e) is the same for all  $j$  and  $t \geq 1$ ; and part (f) is constructed as discussed above. The initial prompt  $\ell_1(1)$  is manually constructed given a scenario  $\xi$  with part (d) being empty [line 3, Alg. 1].

Given  $\ell_j(t)$ , selection of  $s_j(t)$  is represented as an MCQA problem that is solved by the LLM for robot  $j$ . Specifically, given  $\ell_j(t)$  ('question' in MCQA), the LLM  $j$  has to pick decision  $s_j(t)$  among all available ones included in part (a) ('choices' in MCQA). Given any  $s_j(t) \in \mathcal{S}$ , LLMs can provide a score  $g(s_j(t)|\ell_j(t))$ ; the higher the score, the more likely the decision  $s_j(t)$  is a valid next step to positively progress the task [31].<sup>3</sup> To get the scores  $g(s_j(t)|\ell_j(t))$  for all  $s_j(t) \in \mathcal{S}$ , we query the model over all potential decisions  $s_j$  (i.e.,  $S = |\mathcal{S}|$  times in total). Using these scores, a possible approach to select the  $s_j(t)$  is by simply choosing the decision with the highest score, i.e.,  $s_j(t) = \arg \max_{s_j \in \mathcal{S}} g(s_j|\ell_j(t))$ . However, this point-prediction approach is uncertainty-agnostic; note that these scores do not represent calibrated confidence [49]. A much preferred approach would be to generate a set of actions (called, hereafter, *prediction set*), denoted by  $\mathcal{C}(\ell_j(t))$ , that contains the ground truth action with a user-specified high-probability [line 10, Alg. 1]. Hereafter, we assume that such prediction sets are provided. We defer their construction to Section III-D (see (9)) but we emphasize that these sets are critical to achieving desired  $1 - \alpha$  mission completion rates.

Given  $\mathcal{C}(\ell_j(t))$ , we select decisions  $s_j(t)$  as follows. If  $\mathcal{C}(\ell_j(t))$  is singleton, then we select the action included in  $\mathcal{C}(\ell_j(t))$  as it contributes to mission progress with high probability [line 18, Alg. 1].<sup>4</sup> Otherwise, robot  $j$  seeks assistance from its teammates asking all robots to select new decisions for time  $t$  as per a different order  $\mathcal{I}$ . If this does not result in singleton prediction sets, robot  $j$  asks a human operator to select  $s_j(t)$  [lines 11-14, Alg. 1]. The process of seeking assistance is discussed in more detail in Section III-C. Once  $s_j(t)$  is selected, robot  $j$  records  $s_j(t)$  into part (d) of  $\ell_j(t)$ . With slight abuse of notation, we denote this prompt update by  $\ell_{j+1}(t) = \ell_j(t) + s_j(t)$ , where the summation means concatenation of text [line 19, Alg. 1].

Then, robot  $j$  sends the resulting prompt  $\ell_j(t)$  to the next robot  $j+1$  [line 20, Alg. 1]. We repeat the above procedure sequentially over all robots  $j$  as per  $\mathcal{I}$ . This way, we construct the multi-robot action  $\mathbf{s}(t)$  [lines 21-22, Alg. 1]. Once  $\mathbf{s}(t)$  is constructed the current time step is updated to  $t+1$ . The above process is repeated to design  $\mathbf{s}(t+1)$ . This way, we generate a plan  $\tau = \mathbf{s}(1), \dots, \mathbf{s}(t), \dots, \mathbf{s}(H)$  of horizon  $H$ . The robots execute the plan  $\tau$  once it is fully constructed. We assume that  $\tau$  is executed synchronously across the robots; this is a usual assumption in collaborative multi-robot task planning [5], [65].

<sup>3</sup>If the robots do not share the same LLM model, then  $g(s_j(t)|\ell_j(t))$  should be replaced by  $g_j(s_j(t)|\ell_j(t))$  throughout the paper.

<sup>4</sup>By construction of the prediction sets, this action coincides with  $s_j(t) = \arg \max_{s_j \in \mathcal{S}} g(s_j|\ell_j(t))$ ; see Section III-D.

**Remark 3.1 (Unknown/Dynamic Environments):** To relax the assumption of known/static environments, at every time step  $t$ , the action  $\mathbf{s}(t)$  should be executed as soon as it is computed. This execution requires the robots to possess sensor-based controllers  $\mathbf{u}_j$  enabling them to implement  $\mathbf{s}(t)$  in unknown and dynamic environments. Once executed, part (b) in the prompt should be updated as per sensor feedback to account e.g., for new or any missing objects.

**Remark 3.2 (Token Efficiency Benefits):** Algorithm 1, designs the multi-robot action  $\mathbf{s}(t)$  by querying the LLM  $N \cdot S$  times. This is notably more efficient than the centralized approach discussed in Section III-A, where  $S^N$  queries would be required. The reduction to  $N \cdot S$  queries helps in designing multi-robot plans with significantly fewer API calls. This mitigates the exponential increase in API costs associated with the centralized setting as the number of robots grows.

### C. Seeking Assistance

As discussed in Section III-B, if  $\mathcal{C}(\ell_j(t))$  is singleton, then this means that the LLM is sufficiently certain that the decision  $s_j(t)$  included in  $\mathcal{C}(\ell_j(t))$  will contribute to making mission progress. Otherwise, the corresponding robot  $j$  should seek assistance in the following two ways [lines 11-14, Alg. 1]. First, robot  $j$  generates a new order  $\mathcal{I}$  which is forwarded to all robots along with a message to redesign  $\mathbf{s}(t)$  from scratch, as per the new ordered set  $\mathcal{I}$  [lines 11-13, Alg. 1].<sup>5</sup> We iterate over various ordered sets  $\mathcal{I}$  until singleton prediction sets are generated for all robots. Interestingly, our empirical analysis has shown that  $\mathcal{I}$  can potentially affect the size of prediction sets even though this change affects primarily only part (f) in the constructed prompts; see Section V. We remark that this step can significantly increase the number of API calls and the associated costs, and, therefore, it may be neglected for large robot teams and sets  $\mathcal{S}$ . The second type of assistance is pursued when a suitable set  $\mathcal{I}$  cannot be found with the next  $W$  attempts, for some user-specified  $W \geq 0$ . In these cases, the robot  $j$  requests help from human operators [lines 13-14, Alg. 1]. Particularly, robot  $j$  presents to a user the set  $\mathcal{C}(\ell_j(t))$  (along with the prompt  $\ell_j(t)$ ) and asks them to choose one action from it. The user either picks an action for the corresponding robot or decides to halt the operation.

### D. Constructing Local Prediction Sets using CP

In this section, we discuss how the prediction sets  $\mathcal{C}(\ell_j(t))$ , introduced in Section III-B, are constructed, given a required task success rate  $1 - \alpha$  (see Problem 1). The MCQA setup allows us to apply conformal prediction (CP) to construct these sets. To illustrate the challenges of their construction, we consider the following cases: (i) single-robot & single-step plans and (ii) multi-robot & multi-step plans.

**Single-robot & Single-step Plans:** Initially, we focus only scenarios with  $N = 1$  and  $H = 1$ . First, we sample  $M$

<sup>5</sup>This does not violate the coverage guarantees in Section III-D, as the distribution is assumed to generate sequences where the order of robots changes over time steps  $t$  (within the same sequence); see Sec. III-D.

independent scenarios from  $\mathcal{D}$ . We refer to these scenarios as calibration scenarios. For each calibration scenario  $i \in \{1, \dots, M\}$ , we construct its equivalent prompt  $\ell_{j,\text{calib}}^i$  associated with (the single) robot  $j$ . For each prompt, we (manually) compute the ground truth plan  $\tau_{\text{calib}}^i = s_{j,\text{calib}}^i(1)$  accomplishing this task. We assume that there exists a unique correct decision  $s_{j,\text{calib}}^i$  for each  $\ell_{j,\text{calib}}^i$ ; however, by following similar steps as in [49], the following analysis can be extended to cases where this assumption does not hold. Hereafter, we drop the dependence of the robot decisions and prompts on the time step, since we consider single-step plans. This way we construct a calibration dataset  $\mathcal{M} = \{(\ell_{j,\text{calib}}^i, \tau_{\text{calib}}^i)\}_{i=1}^M$ .

Consider a new scenario drawn from  $\mathcal{D}$ , called validation/test scenario. We convert this scenario into its equivalent prompt  $\ell_{j,\text{test}}$ . Since the calibration and the validation scenario are i.i.d., CP can generate a prediction set  $\mathcal{C}(\ell_{j,\text{test}})$  of decisions  $s_j$  containing the correct one, denoted by  $s_{j,\text{test}}$ , with probability greater than  $1 - \alpha$ , i.e.,

$$P(s_{j,\text{test}} \in \mathcal{C}(\ell_{j,\text{test}})) \geq 1 - \alpha, \quad (1)$$

where  $\alpha \in [0, 1]$  is user-specified. To generate  $\mathcal{C}(\ell_{j,\text{test}})$ , CP first uses the LLM's confidence  $g$  to compute the set of non-conformity scores (NCS)  $\{r^i = 1 - g(s_{j,\text{calib}}^i \mid \ell_{j,\text{calib}}^i)\}_{i=1}^M$  over the calibration set. The higher the score is, the less each calibration point conforms to the data used for training the LLM. Then we perform calibration by computing the  $\frac{(M+1)(1-\alpha)}{M}$  empirical quantile of  $r_1, \dots, r_M$  denoted by  $q$ . Using  $q$ , CP constructs the prediction set

$$\mathcal{C}(\ell_{j,\text{test}}) = \{s_j \in \mathcal{S} \mid g(s_j \mid \ell_{j,\text{test}}) > 1 - q\}, \quad (2)$$

that includes all decisions that the model is at least  $1 - q$  confident in. This prediction set is used to select decisions as per Section III-B for single-robot single-step tasks. By construction of the prediction sets the decision  $s_j = \arg \max_{s_j \in \mathcal{S}} g(s_j \mid \ell_{j,\text{test}})$  belongs to  $\mathcal{C}(\ell_{j,\text{test}})$ .

**Multi-robot & Multi-step Plans:** Next, we generalize the above result to the case where  $N \geq 1$  and  $H \geq 1$ . Here we cannot apply directly (1)-(2) to compute individual sets  $\mathcal{C}(\ell_{j,\text{test}}(t))$  for each robot, as this violates the i.i.d. assumption required to apply CP. Particularly, the distribution of prompts  $\ell_{j,\text{test}}(t)$  depends on the previous prompts i.e., the multi-robot decisions at  $t' < t$  as well as the decisions of robots  $1, \dots, j-1$  at time  $t$ . Inspired by [49], we address this challenge by (i) lifting the data to sequences, and (ii) performing calibration at the sequence level using a carefully designed NCS.

We sample  $M \geq 1$  independent calibration scenarios from  $\mathcal{D}$ . Each scenario corresponds to various tasks  $\phi_i$ , numbers of robots  $N_i$ , and mission horizons  $H_i$ . Each task  $\phi_i$  is broken into a sequence of  $T_i = H_i \cdot N_i \geq 1$  prompts defined as in Section III-B. This sequence of  $T_i$  prompts is denoted by

$$\bar{\ell}_{\text{calib}}^i = \underbrace{\ell_{1,\text{calib}}^i(1), \dots, \ell_{j,\text{calib}}^i(1), \dots, \ell_{N_i,\text{calib}}^i(1), \dots}_{t=1},$$

$$\underbrace{\ell_{1,\text{calib}}^i(t'), \dots, \ell_{j,\text{calib}}^i(t'), \dots, \ell_{N_i,\text{calib}}^i(t'), \dots}_{t=t'}$$

$$\underbrace{\ell_{1,\text{calib}}^i(H_i), \dots, \ell_{j,\text{calib}}^i(H_i), \dots, \ell_{N_i,\text{calib}}^i(H_i)}_{t=H_i}. \quad (3)$$

where, by construction, each prompt  $\bar{\ell}_{\text{calib}}^i$  contains a history of ground truth decisions made so far. We define the corresponding sequence of ground truth decisions as:<sup>6</sup>

$$\begin{aligned} \tau_{\text{calib}}^i = & \underbrace{s_{1,\text{calib}}(1), \dots, s_{j,\text{calib}}(1), \dots, s_{N_i,\text{calib}}(1), \dots}_{=s_{\text{calib}}(1)} \\ & \underbrace{s_{1,\text{calib}}(t'), \dots, s_{j,\text{calib}}(t'), \dots, s_{N_i,\text{calib}}(t'), \dots}_{=s_{\text{calib}}(t')} \\ & \underbrace{s_{1,\text{calib}}(H_i), \dots, s_{j,\text{calib}}(H_i), \dots, s_{N_i,\text{calib}}(H_i)}_{=s_{\text{calib}}(H_i)}. \end{aligned} \quad (4)$$

This gives rise to a calibration set  $\mathcal{M} = \{(\bar{\ell}_{\text{calib}}^i, \tau_{\text{calib}}^i)\}_{i=1}^M$ . As before, we assume that each context  $\bar{\ell}_{\text{calib}}^i$  has a unique correct plan  $\tau_{\text{calib}}^i$ . We denote by  $\bar{\ell}_{\text{calib}}^i(k)$  and  $\tau_{\text{calib}}^i(k)$  the  $k$ -th entry in  $\bar{\ell}_{\text{calib}}^i$  and  $\tau_{\text{calib}}^i$ , respectively, where  $k \in \{1, \dots, T_i\}$ . Note that the iterations  $k$  are different from the time steps  $t \in \{1, \dots, H_i\}$ . Each iteration  $k$  points to a specific robot index  $j$  and time  $t$ .

Next, for each calibration sequence, we define the NCS similarly to the single-robot-single-step plan case. Specifically, the NCS of the  $i$ -th calibration sequence, denoted by  $\bar{r}_i$ , is computed based on the lowest NCS over  $k \in \{1, \dots, T_i\}$ , i.e.,

$$\bar{r}_i = 1 - \bar{g}(\tau_{\text{calib}}^i \mid \bar{\ell}_{\text{calib}}^i), \quad (5)$$

where

$$\bar{g}(\tau_{\text{calib}}^i \mid \bar{\ell}_{\text{calib}}^i) = \min_{k \in \{1, \dots, T_i\}} g(s_{\text{calib}}^i(k) \mid \bar{\ell}_{\text{calib}}^i(k)). \quad (6)$$

Consider a new validation scenario drawn from  $\mathcal{D}$  associated with a task  $\phi_{\text{test}}$  that is defined over  $N_{\text{test}}$  robots and horizon  $H_{\text{test}}$  corresponding to a sequence of prompts

$$\bar{\ell}_{\text{test}} = \bar{\ell}_{\text{test}}(1), \dots, \bar{\ell}_{\text{test}}(k), \dots, \bar{\ell}_{\text{test}}(T_{\text{test}}),$$

where  $T_{\text{test}} = H_{\text{test}} \cdot N_{\text{test}}$ . Using the set  $\mathcal{M}$ , CP can generate a prediction set  $\bar{\mathcal{C}}(\bar{\ell}_{\text{test}})$  of plans  $\tau$ , containing the correct one, denoted by  $\tau_{\text{test}}$ , with probability greater than  $1 - \alpha$ , i.e.,

$$P(\tau_{\text{test}} \in \bar{\mathcal{C}}(\bar{\ell}_{\text{test}})) \geq 1 - \alpha. \quad (7)$$

The prediction set  $\bar{\mathcal{C}}(\bar{\ell}_{\text{test}})$  is defined as:

$$\bar{\mathcal{C}}(\bar{\ell}_{\text{test}}) = \{\tau \mid \bar{g}(\tau \mid \bar{\ell}_{\text{test}}) > 1 - \bar{q}\}, \quad (8)$$

where  $\bar{q}$  is the  $\frac{(M+1)(1-\alpha)}{M}$  empirical quantile of  $\bar{r}_1, \dots, \bar{r}_M$ . The size of the prediction sets can be used to evaluate

<sup>6</sup>The distribution  $\mathcal{D}$  over scenarios induces a distribution over data sequences (3) [49]. These data sequences are equivalent representations of the sampled scenarios augmented with the ground truth decisions. Observe that in these sequences the order of robot indices is determined by an ordered set  $\mathcal{I}_i$  (generated by the induced distribution over the data sequences). For ease of notation, in this section, we assume that the ordered set is defined as  $\mathcal{I}_i = \{1, \dots, N_i\}$  and  $\mathcal{I}_{\text{test}} = \{1, \dots, N_{\text{test}}\}$  for all calibration and validation sequences, respectively, and for all time steps  $t$ . However, in general, we remark that these ordered sets do not need to be the same across the calibration sequences  $i$  and they can also change across the time steps  $t$  within the  $i$ -th calibration sequence. The same holds for the test sequence; this will be used in Section III-C.

uncertainty of the LLM. Specifically, if  $\bar{\mathcal{C}}(\bar{\ell}_{\text{test}})$  is singleton then this means that the LLM is certain with probability at least  $1 - \alpha$  that the designed multi-robot plan accomplishes the assigned task.

On-the-fly and Local Construction: Notice that  $\bar{\mathcal{C}}(\bar{\ell}_{\text{test}})$  in (8) is constructed after the entire sequence  $\bar{\ell}_{\text{test}} = \bar{\ell}_{\text{test}}(1), \dots, \bar{\ell}_{\text{test}}(T_{\text{test}})$  is obtained. However, at test time, we do not see the entire sequence of prompts all at once; instead, the contexts  $\bar{\ell}_{\text{test}}(k)$  are revealed sequentially over iterations  $k$ , as the robots pick their actions. Thus, next we construct the prediction set  $\bar{\mathcal{C}}(\bar{\ell}_{\text{test}})$  on-the-fly and incrementally, using only the current and past information, as the robots take turns in querying their LLMs for action selection. At every iteration  $k \in \{1, \dots, T\}$ , we construct the local prediction set associated with a robot  $j$  and a time step  $t$ ,

$$\mathcal{C}(\bar{\ell}_{\text{test}}(k)) = \{\tau_{\text{test}}(k) \mid g(\tau_{\text{test}}(k) | \bar{\ell}_{\text{test}}(k)) > 1 - \bar{q}\}, \quad (9)$$

where  $g$  refers to the (uncalibrated) LLM score used in Section III-B. The prediction set  $\mathcal{C}(\bar{\ell}_{\text{test}}(k))$  in (9) should be used by the respective robot  $j$  to select a decision  $s_j(t)$ . Essentially,  $\mathcal{C}(\bar{\ell}_{\text{test}}(k))$  corresponds to the set  $\mathcal{C}(\ell_j(t))$  used in Section III-B and in [line 10, Alg. 1].<sup>7</sup> As it will be shown in Section IV, it holds that  $\bar{\mathcal{C}}(\bar{\ell}_{\text{test}}) = \hat{\mathcal{C}}(\bar{\ell}_{\text{test}})$ , where

$$\hat{\mathcal{C}}(\bar{\ell}_{\text{test}}) = \mathcal{C}(\bar{\ell}_{\text{test}}(1)) \times \dots \times \mathcal{C}(\bar{\ell}_{\text{test}}(k)) \dots \times \mathcal{C}(\bar{\ell}_{\text{test}}(T_{\text{test}})). \quad (10)$$

*Remark 3.3 (Communication Architecture):* Construction of  $\mathcal{C}(\bar{\ell}_{\text{test}}(k))$  is done locally by the corresponding robot  $j$  using only the prompt of the previous robot. As discussed in Section III-B, the latter is needed in order to construct  $\bar{\ell}_{\text{test}}(k)$  and, consequently,  $\mathcal{C}(\bar{\ell}_{\text{test}}(k))$ . Notice that communication can naturally occur in a multi-hop fashion and all-to-all communication is not needed.

*Remark 3.4 (Dataset-Conditional Guarantee):* The probabilistic guarantee in (7) is *marginal* since the probability is over both the sampling of the calibration set  $\mathcal{M}$  and the validation point  $\bar{\ell}_{\text{test}}$ . Thus, a new calibration set is needed for every single test data point  $\bar{\ell}_{\text{test}}$  to ensure the desired coverage level. A dataset-conditional guarantee which holds for a fixed calibration set can also be applied [66].

#### IV. THEORETICAL MISSION SUCCESS RATE GUARANTEES

In this section, we show that the proposed language-based multi-robot planner presented Algorithm 1 achieves user-specified  $1 - \alpha$  mission success rates. To show this, we need first to state the following result; the proofs of the following results are adapted from [49].

*Proposition 4.1:* The prediction set  $\bar{\mathcal{C}}(\bar{\ell}_{\text{test}})$  defined in (8) is the same as the on-the-fly constructed prediction set  $\hat{\mathcal{C}}(\bar{\ell}_{\text{test}})$  defined in (10), i.e.,  $\bar{\mathcal{C}}(\bar{\ell}_{\text{test}}) = \hat{\mathcal{C}}(\bar{\ell}_{\text{test}})$ .

*Proof:* It suffices to show that if a multi-robot plan  $\tau$  belongs to  $\bar{\mathcal{C}}(\bar{\ell}_{\text{test}})$  then it also belongs to  $\hat{\mathcal{C}}(\bar{\ell}_{\text{test}})$  and vice-versa. First, we show that if  $\tau \in \bar{\mathcal{C}}(\bar{\ell}_{\text{test}})$  then  $\tau \in \hat{\mathcal{C}}(\bar{\ell}_{\text{test}})$ . Since  $\tau \in \bar{\mathcal{C}}(\bar{\ell}_{\text{test}})$ , then we have that  $\min_{k \in \{1, \dots, T_{\text{test}}\}} g(\tau(k) | \bar{\ell}_{\text{test}}(k)) >$

<sup>7</sup>For instance, the set  $\mathcal{C}(\bar{\ell}_{\text{test}}(k))$  with  $k = N_{\text{test}} + 1$  refers to the prediction set of robot  $\mathcal{I}(1)$  at time  $t = 2$ .

$1 - \bar{q}$  due to (6). This means that  $g(\tau(k) | \bar{\ell}_{\text{test}}(k)) > 1 - \bar{q}$ , for all  $k \in \{1, \dots, T_{\text{test}}\}$ . Thus,  $\tau(k) \in \mathcal{C}(\bar{\ell}_{\text{test}}(k))$ , for all  $k \in \{1, \dots, T_{\text{test}}\}$ . By definition of  $\hat{\mathcal{C}}(\bar{\ell}_{\text{test}})$  in (10), this implies that  $\tau \in \hat{\mathcal{C}}(\bar{\ell}_{\text{test}})$ . These steps hold in the other direction too showing that if  $\tau \in \hat{\mathcal{C}}(\bar{\ell}_{\text{test}})$  then  $\tau \in \bar{\mathcal{C}}(\bar{\ell}_{\text{test}})$ . ■

*Theorem 4.2 (Mission Success Rate):* Assume that prediction sets are constructed causally with coverage level  $1 - \alpha$  and that the robots seek help from a user whenever the prediction set  $\mathcal{C}(\bar{\ell}_{\text{test}}(k))$  - defined in (9) - is not singleton after  $W$  attempts; see Section III-C. (a) The task completion rate over new test scenarios (and the randomness of the calibration sets) drawn from  $\mathcal{D}$  is at least  $1 - \alpha$ . (b) If  $\bar{g}(\tau | \bar{\ell}_{\text{test}})$  models true conditional probabilities, the average size of the sets  $\bar{\mathcal{C}}(\bar{\ell}_{\text{test}})$  is minimized among possible prediction schemes that achieve  $1 - \alpha$  completion rate.

*Proof:* (a) To show this result, we consider the following cases. Case I: We have that  $|\mathcal{C}(\bar{\ell}_{\text{test}}(k))| = 1, \forall k \in \{1, \dots, T_{\text{test}}\}$  (with or without the robots ‘helping’ each other) and  $\tau_{\text{test}} \in \hat{\mathcal{C}}(\bar{\ell}_{\text{test}})$  where  $\tau_{\text{test}}$  is the ground truth plan and  $\hat{\mathcal{C}}(\bar{\ell}_{\text{test}})$  is defined as in (10). In this case, the robots will select the correct plan. Case II: We have that  $|\mathcal{C}(\bar{\ell}_{\text{test}}(k))| > 1, \forall k \in \{1, \dots, T_{\text{test}}\}$  and  $\tau_{\text{test}} \in \hat{\mathcal{C}}(\bar{\ell}_{\text{test}})$ . In this case, the robots will select the correct plan assuming users who faithfully provide help. Case III: We have that  $\tau_{\text{test}} \notin \hat{\mathcal{C}}(\bar{\ell}_{\text{test}})$ . The latter means that there exists at least one iteration  $k$  such that  $\tau_{\text{test}}(k) \notin \mathcal{C}(\bar{\ell}_{\text{test}}(k))$ . In this case, the robots will compute an incorrect plan. Observe that the probability that either Case I or II will occur is equivalent to the probability  $P(\tau_{\text{test}} \in \hat{\mathcal{C}}(\bar{\ell}_{\text{test}}))$ . Due to Prop. 4.1 and (7), we have that  $P(\tau_{\text{test}} \in \hat{\mathcal{C}}(\bar{\ell}_{\text{test}})) \geq 1 - \alpha$ . Thus, either of Case I and II will occur with probability that is at least equal to  $1 - \alpha$ . Since Cases I-III are mutually and collectively exhaustive, we conclude that the probability that Case III will occur is less than  $\alpha$ . This implies that the mission success rate is at least  $1 - \alpha$ . (b) This result holds directly due to Theorem 1 in [67]. ■

#### V. EXPERIMENTS

To illustrate the performance of the proposed planner, we conduct extensive comparative experiments considering home service robot tasks on the AI2THOR simulator [68]. In Section V-A, we show empirically that our proposed planner achieves better planning performance than recent centralized and decentralized LLM-based planners (even when the help-request module is deactivated). In Section V-B, we empirically validate the theoretical results shown in Section IV. In Section V-C, we demonstrate how assistance from robot teammates can potentially help robots make more certain decisions. In all case studies, we pick GPT-3.5 [69] as the LLM for all robots.

##### A. Comparative Experiments

**Setup:** We consider home service robot tasks defined over the following 12 semantic objects with labels  $\mathcal{O} = \{\text{Apple, Kettle, Tomato, Bread, Potato, Knife}\}$ . The set of actions is defined as  $\mathcal{A} = \{\text{go to, grab object, put object down, open door, remain idle}\}$ .

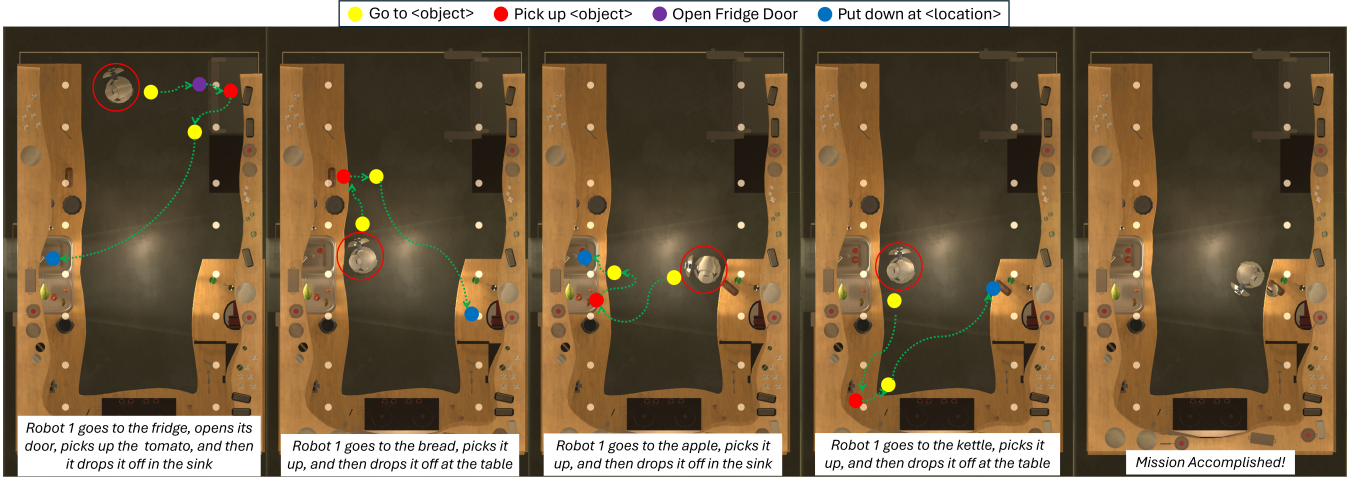


Fig. 4: Case Study I: Execution of a single-robot plan for the mission: ‘Deliver a tomato and an apple to the sink. Also, deliver the kettle and the bread to the table’. Each snapshot illustrates a segment of the robot’s plan to achieve each sub-task.

The action ‘remain idle’ is useful when all sub-tasks in  $\phi$  have been assigned to other robots or when the task has been accomplished before the given horizon  $H$ . The number of decisions that the LLM can pick from is  $|\mathcal{S}| = 28$ . Recall that  $\mathcal{S}$  is constructed using  $\mathcal{A}$  and all objects/locations in the environment where actions in  $\mathcal{A}$  can be applied. We also construct a distribution  $\mathcal{D}$  so that it can generate a scenario  $\xi$  with  $N = 1$ ,  $N = 3$ ,  $N = 10$ , or  $N = 15$  robots, with probabilities 0.5, 0.2, 0.2, and 0.1, respectively. Within each category, (i) the number of sub-tasks in  $\phi$  falls within a specific range; (ii) the horizon  $H$  is fixed. Given one of these four categories, the number of sub-tasks is selected randomly from the corresponding predefined range and the sub-tasks are selected randomly from a pre-constructed set.

**Baselines:** We compare Alg. 1 against a recent decentralized (DMAS) and a centralized (CMAS) multi-robot planner proposed in [40]. We select [40] due to its token efficiency and scalability properties as shown in the empirical studies of that work. DMAS assigns an LLM agent to each robot in the team. At every time step  $t$ , the LLM agents engage in dialogue rounds to pick their corresponding decisions  $s_j(t)$ . CMAS on the other hand considers a single LLM that is responsible for generating the multi-robot decision  $s(t)$ . A major difference between our proposed method and these baselines is that the latter do not employ the MCQA framework while in DMAS the robots may engage in endless dialogues. In our comparisons, we select the planning accuracy as the main performance metric, defined as the percentage of scenarios where a planner generates a feasible plan accomplishing the assigned task. To compute this accuracy, we manually check the correctness of the designed plans. We also discuss trade offs between token efficiency and planning accuracy. To make comparisons fair we have applied all algorithms under the following settings: (i) All methods share the same prompt structure and select a decision from the same set  $\mathcal{S}$ . (ii) All methods terminate after a pre-defined mission horizon  $H$ . Cases where a planner fails to compute a plan within  $H$  time steps are considered incorrect for all methods. (iii) We remove altogether the

CP component from our planner (since it does not exist in the baselines). The latter means that our planner always picks the action  $s_j(t) = \arg \max_{s \in \mathcal{S}} g(s|\ell_j(t))$  for all robots  $j$  and time steps  $t$ . Comparisons against the centralized method discussed in Section III-A were not possible due to its prohibitively high API costs; see also Remark 5.1. We draw 110 i.i.d. scenarios  $\xi$  from the distribution  $\mathcal{D}$ . In what follows, we group the generated scenarios based on the category (i.e., number of robots) they belong to and we report the accuracy of our planner and the baselines.

**Case Study I:** We consider 27 scenarios with single-robot tasks (i.e.,  $N = 1$ ) defined over four sub-tasks and at most one safety requirement. Each sub-task requires moving a specific semantic object to a desired location. The safety constraint requires the robot to avoid approaching or grabbing specific objects. For instance, a task may require the robot to move two tomatoes and one potato from the fridge to the kitchen counter (three sub-tasks), put the bread in the microwave (one sub-task) and to never grab the knife located on the kitchen counter (safety constraint). Other missions may offer to the robots multiple possible destinations for the objects. We select as maximum horizon  $H = 15$  for all scenarios considered in this case study. The proposed planner designed correct plans in 25 cases, i.e., the accuracy was 92.5%. CMAS and DMAS achieved an accuracy of 37.2%. Notice that when  $N = 1$ , the two baselines trivially share the same planning scheme and, similarly, Alg. 1 and [49] are exactly the same. The average horizon  $\bar{H}$  for our planner, CMAS, and DMAS, across all successful scenarios, is 12, 13, and 13, respectively. A robot plan designed for one of the considered scenarios is shown in Fig. 4.

**Case Study II:** We consider 55 scenarios with tasks  $\phi$  defined over  $N = 3$  robots and four to eight sub-tasks and at most one safety constraint. Notice that since the minimum number of sub-tasks in  $\phi$  is larger than  $N$ , this means that at least one robot will have to eventually accomplish at least one sub-task. Recall from Section II that these sub-tasks are not pre-assigned to the robots; instead, the LLM should compute both a feasible task assignment and a mission plan. The

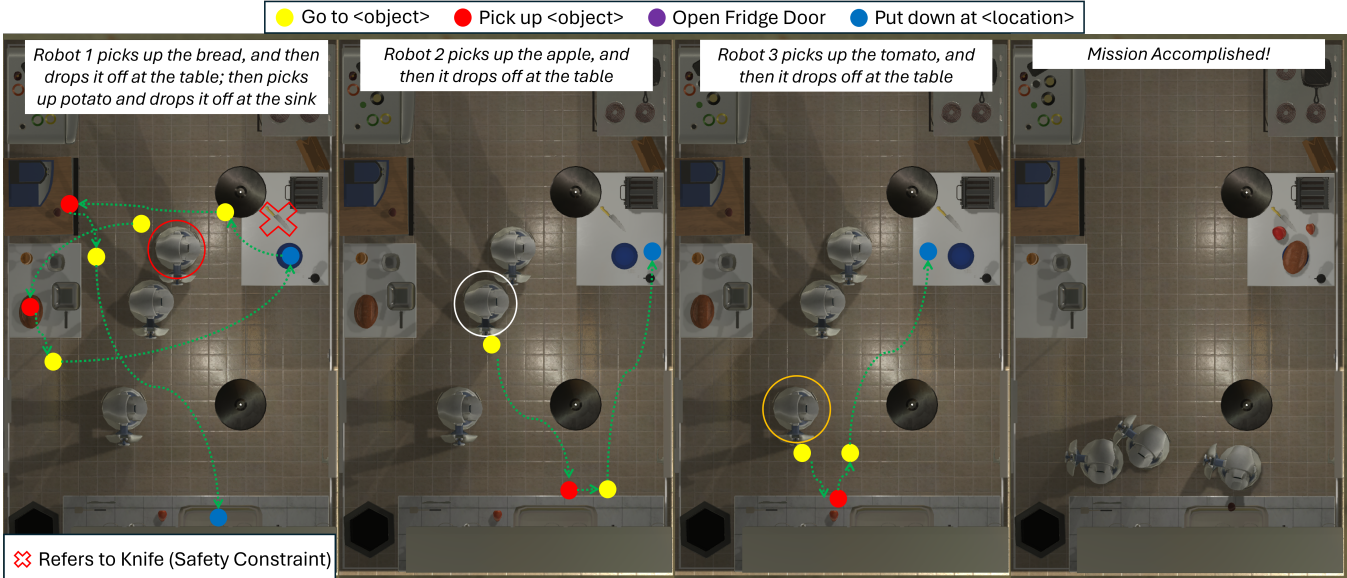


Fig. 5: Case Study II: Execution of a multi-robot plan for the mission: ‘Deliver the bread, apple and tomato to the table; Deliver the potato to the sink. Also, Robot 1 should never pick up a knife’. The first three snapshots left illustrate the plans generated by each robot to achieve certain sub-tasks of the mission. The fourth snapshot shows the environment when all the sub-tasks are completed.

maximum horizon is  $H = 9$  in this case. The accuracy of our planner, CMAS, and DMAS is 83.3%, 30.9%, and 27.3%, respectively. The average horizon  $\bar{H}$  for all methods, across all successful scenarios, is 7 respectively. Observe that unlike the baselines, the performance of our method has not dropped significantly despite the increase in the number of robots and the task complexity. We believe that this performance drop is attributed to the larger number of robots considered here. Snapshots demonstrating a robot plan synthesized for a three-robot scenario are shown in Fig. 5.

**Case Study III:** Next, we consider scenarios over larger robot teams. Specifically, we consider 20 scenarios associated with  $N = 10$  robots and missions  $\phi$  involving four to eight sub-tasks and at most one safety constraint. Notice here that the number of robots is larger than the maximum number of sub-tasks in  $\phi$ . This means that there should be robots with no tasks assigned by the LLM. The maximum horizon is  $H = 4$  in this case. The accuracy of our planner, CMAS, and DMAS is 95%, 60%, and 5%, respectively. Despite the larger number of robots in this case study, compared to the previous one, our planner achieves high accuracy. Notably, the planning accuracy of our planner and CMAS has improved compared to Case Study II. We attribute this to the shorter horizon  $\bar{H}$  required in this case study compared to the previous one. In fact, the average horizon  $\bar{H}$  for all methods, across all successful scenarios, is 4 time steps. This shorter horizon is due to the fact that Case Study III involves a larger number of robots accomplishing the same number of sub-tasks as in Case Study II.

**Case Study IV:** In our final case study, we consider 8 scenarios that include  $N = 15$  robots and missions with ten sub-tasks and at most one safety constraint. We select  $H = 4$  as a maximum horizon. The accuracy of our planner, CMAS, and DMAS is 87.5%, 25%, and 0%, respectively. The average horizon  $\bar{H}$  for all methods is 4. Observe that

even though the horizons  $\bar{H}$  in the previous and the current case study are similar, the performance of the baselines has dropped significantly possibly due to the larger number  $N$  of robots as well as the larger number of associated sub-tasks.

**Summary of Comparisons:** The above empirical results show that the performance gap between our method and the baselines increases significantly as the scenario complexity increases, where the latter is determined primarily by the horizon  $\bar{H}$ , the robot team size  $N$ , and the number of sub-tasks in  $\phi$ . Specifically, as  $\bar{H}$  increases (e.g., due to a low ratio of the number of robots over the number of sub-tasks), the performance of the baselines drops; see e.g., Case Study I and II. Also, for scenarios associated with similar values for  $\bar{H}$ , the performance of the baselines tends to drop as the number of robots and sub-tasks increase; see Case Study III-IV. The accuracy of the proposed planner seems to be more robust to such variations. We attribute this empirical performance improvement to the MCQA framework, as it attempts to eliminate hallucinations. To the contrary, CMAS and DMAS require the employed LLMs to generate new tokens to design multi-robot plans increasing the risk of hallucinations. Notably, CMAS achieves better planning accuracy than DMAS which is also consistent with the results presented in [40]. We would like to highlight again that Alg. 1 can achieve desired mission success rates (see Section V-B), a capability that is missing in existing LLM-based multi-robot planners including the inspiring work in [40].

*Remark 5.1 (Token Efficiency vs Planning Accuracy):* As demonstrated earlier, the proposed planner achieves higher planning accuracy than CMAS. However, this increased accuracy comes at the cost of lower token efficiency (i.e., a larger number of API calls). Specifically, CMAS requires only one API call to design  $\mathbf{s}(t)$  while our planner requires  $N \cdot |\mathcal{S}|$  calls (assuming  $W = 0$ ). On the other hand, DMAS requires  $J \geq N$  calls, where  $J$  is

the (a priori unknown) number of dialogue rounds needed to complete the construction of the multi-robot action. We also emphasize that our method is significantly more token efficient than the centralized method discussed in Section III-A, which demands  $|\mathcal{S}|^N$  API calls. For example, when designing  $\mathbf{s}(t)$  for a scenario from Case Studies II, III, and IV, our method requires 84, 280, and 420 API calls, respectively, while the centralized approach would necessitate  $21,952$ ,  $2.962 \cdot 10^{14}$ , and  $5.0977 \cdot 10^{21}$  calls, respectively, resulting in prohibitive API costs even for the design of single-step multi-robot plans.

*Remark 5.2 (Hybrid Planners):* The work in [40] proposes also hybrid frameworks as extensions of CMAS and DMAS. Specifically, once CMAS generates a plan, LLMs are employed to detect and resolve conflicts in a centralized or decentralized way. These conflicts include robot collisions that may occur during the plan execution, as well as the assignment of actions that do not belong to the action set. Our planner prevents the latter from happening due to MCQA framework. Although our proposed algorithm can also be integrated with similar frameworks to prevent collisions during the plan execution, this aspect is beyond the scope of this work.

### B. Empirical Validation of Mission Success Rates

The average mission success rate/planning accuracy of our planner across the 110 scenarios considered in Section IV is 87.9%. In this section, we empirically validate the mission success rates discussed in Section IV, i.e., we investigate if we can increase the mission success rate to a desired level  $1 - \alpha$  ( $> 87.9\%$ ) by allowing the planner to ask for help when needed; see Section IV. For each validation scenario considered in Section IV, we sample 30 calibration sequences from  $\mathcal{D}$  used to construct prediction sets. Then, for each scenario, we compute the plan using Alg. 1 with  $W = 0$  (to minimize API calls) and (manually) check if the robot plan is the ground truth plan. We compute the ratio of how many of the corresponding 110 generated plans are the ground truth ones. We repeat this 50 times. The average ratio across all experiments is the (empirical) mission success rate. When  $1 - \alpha = 0.90$  and  $1 - \alpha = 0.95$ , the mission success rate was 94.59% and 96.57% respectively, validating Theorem 4.2. When  $1 - \alpha = 0.90$  and  $1 - \alpha = 0.95$ , the average percentage of local prediction sets  $\mathcal{C}(\ell_{\text{test}}(k))$  that were singletons was 95.56% and 91.90%, respectively. This equivalently means that when  $1 - \alpha = 0.90$  and  $1 - \alpha = 0.95$ , help was requested in making 4.44% and 8.1% of all decisions  $s_j(t)$ , respectively. As expected, the frequency of help requests increases as the desired mission success rate increases.

### C. Asking for Help from Robot Teammates

In this section, we select five scenarios from Section V-B, with  $N = 3$ , where non-singleton prediction sets were constructed. We show that re-computing  $\mathbf{s}(t)$  using a different set  $\mathcal{I}$  can potentially result in smaller prediction sets. In each of these scenarios, we select  $W = 1$ , and we observed that two scenarios switched to singleton prediction

sets. In the first scenario, the task  $\phi$  requires the robots to move a tomato and a water bottle to the sink, put the kettle to stove burner, and the bread at the table. We initialize the ordered set of robot indices as  $\mathcal{I} = \{1, 2, 3\}$ . In this scenario, the bottle of water is inside the closed fridge and, therefore, grabbing the bottle requires first opening the fridge door. The prediction set  $\mathcal{C}(\ell_1(1))$  for the robot  $\mathcal{I}(1) = 1$  at  $t = 1$  is non-singleton and contains the following actions: (go to location of water bottle), (go to the location of the fridge). In this case, robot 1 (randomly) generates a new ordered set:  $\mathcal{I}' = \{2, 1, 3\}$  and asks all robots to select their decisions as per  $\mathcal{I}'$ . Thus, the  $\mathcal{I}'(1) = 2$  will select first an action. In this case, the corresponding prediction set is singleton defined as (go to the location of the fridge). Notice that if a singleton prediction set cannot be constructed within  $W$  different sets  $\mathcal{I}$ , then help from a user will be requested. Similar observations were made in the second scenario requiring the robots to move multiple objects at desired locations. We note again here that changing the set  $\mathcal{I}$  may not always result in smaller prediction sets, as this minimally affects the prompts.

## VI. CONCLUSIONS, LIMITATIONS, AND FUTURE WORK

This paper proposed a new decentralized planner for language-instructed robot teams. We showed both theoretically and empirically that the proposed planner is capable of achieving desired mission success rates while asking for help from users only when necessary. We also provided comparative experiments showing that it outperforms recent LLM-based multi-robot planners in terms of planning accuracy even when the help-mode is deactivated. One of the main limitations of this work is that it assumes that all robot skills can be executed perfectly. However, this may not hold in practice violating our theoretical mission success rate guarantees. Inspired by [31], our future work will focus on relaxing this assumption and providing real-world grounding.

## REFERENCES

- [1] B. Schlotfeldt, D. Thakur, N. Atanasov, V. Kumar, and G. J. Pappas, “Anytime planning for decentralized multirobot active information gathering,” *IEEE Robotics and Automation Letters*, vol. 3, no. 2, pp. 1025–1032, 2018.
- [2] Y. Kantaros and M. M. Zavlanos, “Distributed communication-aware coverage control by mobile sensor networks,” *Automatica*, vol. 63, pp. 209–220, 2016.
- [3] W. Gosrich, S. Mayya, R. Li, J. Paulos, M. Yim, A. Ribeiro, and V. Kumar, “Coverage control in multi-robot systems via graph neural networks,” in *2022 International Conference on Robotics and Automation (ICRA)*. IEEE, 2022, pp. 8787–8793.
- [4] K. Elimelech, L. E. Kavraki, and M. Y. Vardi, “Efficient task planning using abstract skills and dynamic road map matching,” in *The International Symposium of Robotics Research*. Springer, 2022, pp. 487–503.
- [5] Y. Kantaros and M. M. Zavlanos, “Stylus\*: A temporal logic optimal control synthesis algorithm for large-scale multi-robot systems,” *The International Journal of Robotics Research*, vol. 39, no. 7, pp. 812–836, 2020.
- [6] M. Turpin, N. Michael, and V. Kumar, “Capt: Concurrent assignment and planning of trajectories for multiple robots,” *The International Journal of Robotics Research*, vol. 33, no. 1, pp. 98–112, 2014.
- [7] P. Pianpak, T. C. Son, P. O. Toups Dugas, and W. Yeoh, “A distributed solver for multi-agent path finding problems,” in *Proceedings of the First International Conference on Distributed Artificial Intelligence*, 2019, pp. 1–7.

[8] A. Fang and H. Kress-Gazit, “Automated task updates of temporal logic specifications for heterogeneous robots,” in *2022 International Conference on Robotics and Automation (ICRA)*. IEEE, 2022, pp. 4363–4369.

[9] V. Vasilopoulos and D. E. Koditschek, “Reactive navigation in partially known non-convex environments,” in *International Workshop on the Algorithmic Foundations of Robotics*. Springer, 2018, pp. 406–421.

[10] S. Karaman and E. Frazzoli, “Sampling-based algorithms for optimal motion planning,” *The International Journal of Robotics Research*, vol. 30, no. 7, pp. 846–894, 2011.

[11] L. E. Kavraki, P. Svestka, J.-C. Latombe, and M. H. Overmars, “Probabilistic roadmaps for path planning in high-dimensional configuration spaces,” *IEEE transactions on Robotics and Automation*, vol. 12, no. 4, pp. 566–580, 1996.

[12] C. R. Garrett, R. Chitnis, R. Holladay, B. Kim, T. Silver, L. P. Kaelbling, and T. Lozano-Pérez, “Integrated task and motion planning,” *Annual review of control, robotics, and autonomous systems*, vol. 4, pp. 265–293, 2021.

[13] L. Antonyshyn, J. Silveira, S. Givigi, and J. Marshall, “Multiple mobile robot task and motion planning: A survey,” *ACM Computing Surveys*, vol. 55, no. 10, pp. 1–35, 2023.

[14] C. Baier and J.-P. Katoen, *Principles of model checking*. MIT press Cambridge, 2008, vol. 26202649.

[15] R. S. Sutton and A. G. Barto, *Reinforcement learning: An introduction*. MIT press, 2018.

[16] J. Achiam, S. Adler, S. Agarwal, L. Ahmad, I. Akkaya, F. L. Aleman, D. Almeida, J. Alten Schmidt, S. Altman, S. Anadkat *et al.*, “Gpt-4 technical report,” *arXiv preprint arXiv:2303.08774*, 2023.

[17] H. Touvron, L. Martin, K. Stone, P. Albert, A. Almahairi, Y. Babaei, N. Bashlykov, S. Batra, P. Bhargava, S. Bhosale *et al.*, “Llama 2: Open foundation and fine-tuned chat models,” *arXiv preprint arXiv:2307.09288*, 2023.

[18] D. Driess, F. Xia, M. S. Sajjadi, C. Lynch, A. Chowdhery, B. Ichter, A. Wahid, J. Tompson, Q. Vuong, T. Yu *et al.*, “Palm-e: An embodied multimodal language model,” *arXiv preprint arXiv:2303.03378*, 2023.

[19] I. Singh, V. Blukis, A. Mousavian, A. Goyal, D. Xu, J. Tremblay, D. Fox, J. Thomason, and A. Garg, “Progpprompt: Generating situated robot task plans using large language models,” in *IEEE International Conference on Robotics and Automation (ICRA)*, 2023, pp. 11 523–11 530.

[20] J. Liang, W. Huang, F. Xia, P. Xu, K. Hausman, B. Ichter, P. Florence, and A. Zeng, “Code as policies: Language model programs for embodied control,” in *IEEE International Conference on Robotics and Automation (ICRA)*, 2023, pp. 9493–9500.

[21] D. Shah, B. Osiński, S. Levine *et al.*, “Lm-nav: Robotic navigation with large pre-trained models of language, vision, and action,” in *Conference on Robot Learning*. PMLR, 2023, pp. 492–504.

[22] Y. Xie, C. Yu, T. Zhu, J. Bai, Z. Gong, and H. Soh, “Translating natural language to planning goals with large-language models,” *arXiv preprint arXiv:2302.05128*, 2023.

[23] Y. Ding, X. Zhang, C. Paxton, and S. Zhang, “Task and motion planning with large language models for object rearrangement,” *arXiv preprint arXiv:2303.06247*, 2023.

[24] B. Liu, Y. Jiang, X. Zhang, Q. Liu, S. Zhang, J. Biswas, and P. Stone, “Llm+ p: Empowering large language models with optimal planning proficiency,” *arXiv preprint arXiv:2304.11477*, 2023.

[25] J. Wu, R. Antonova, A. Kan, M. Lepert, A. Zeng, S. Song, J. Bohg, S. Rusinkiewicz, and T. Funkhouser, “Tidybot: Personalized robot assistance with large language models,” *arXiv preprint arXiv:2305.05658*, 2023.

[26] A. Zeng, M. Attarian, B. Ichter, K. Choromanski, A. Wong, S. Welker, F. Tombari, A. Purohit, M. Ryoo, V. Sindhwanı *et al.*, “Socratic models: Composing zero-shot multimodal reasoning with language,” *arXiv preprint arXiv:2204.00598*, 2022.

[27] S. Stepputtis, J. Campbell, M. Phielipp, S. Lee, C. Baral, and H. Ben Amor, “Language-conditioned imitation learning for robot manipulation tasks,” *Advances in Neural Information Processing Systems*, vol. 33, pp. 13 139–13 150, 2020.

[28] S. Li, X. Puig, C. Paxton, Y. Du, C. Wang, L. Fan, T. Chen, D.-A. Huang, E. Akyürek, A. Anandkumar *et al.*, “Pre-trained language models for interactive decision-making,” *Advances in Neural Information Processing Systems*, vol. 35, pp. 31 199–31 212, 2022.

[29] W. Huang, F. Xia, T. Xiao, H. Chan, J. Liang, P. Florence, A. Zeng, J. Tompson, I. Mordatch, Y. Chebotar *et al.*, “Inner monologue: Embodied reasoning through planning with language models,” *arXiv preprint arXiv:2207.05608*, 2022.

[30] J. Ruan, Y. Chen, B. Zhang, Z. Xu, T. Bao, G. Du, S. Shi, H. Mao, X. Zeng, and R. Zhao, “Tptu: Task planning and tool usage of large language model-based ai agents,” *arXiv preprint arXiv:2308.03427*, 2023.

[31] M. Ahn, A. Brohan, N. Brown, Y. Chebotar, O. Cortes, B. David, C. Finn, C. Fu, K. Gopalakrishnan, K. Hausman *et al.*, “Do as i can, not as i say: Grounding language in robotic affordances,” *arXiv preprint arXiv:2204.01691*, 2022.

[32] X. Luo, S. Xu, and C. Liu, “Obtaining hierarchy from human instructions: an llms-based approach,” in *CoRL 2023 Workshop on Learning Effective Abstractions for Planning (LEAP)*, 2023.

[33] F. Joublin, A. Ceravola, P. Smirnov, F. Ocker, J. Deigmoeller, A. Bellardinelli, C. Wang, S. Hasler, D. Tanneberg, and M. Gienger, “Copal: Corrective planning of robot actions with large language models,” *arXiv preprint arXiv:2310.07263*, 2023.

[34] Z. Dai, A. Asghariavaskasi, T. Duong, S. Lin, M.-E. Tzes, G. Pappas, and N. Atanasov, “Optimal scene graph planning with large language model guidance,” *arXiv preprint arXiv:2309.09182*, 2023.

[35] Z. Mandi, S. Jain, and S. Song, “Roco: Dialectic multi-robot collaboration with large language models,” *arXiv preprint arXiv:2307.04738*, 2023.

[36] H. Zhang, W. Du, J. Shan, Q. Zhou, Y. Du, J. B. Tenenbaum, T. Shu, and C. Gan, “Building cooperative embodied agents modularly with large language models,” *arXiv preprint arXiv:2307.02485*, 2023.

[37] Y. Talebirad and A. Nadiri, “Multi-agent collaboration: Harnessing the power of intelligent llm agents,” *arXiv preprint arXiv:2306.03314*, 2023.

[38] Z. Liu, W. Yao, J. Zhang, L. Xue, S. Heinecke, R. Murthy, Y. Feng, Z. Chen, J. C. Niebles, D. Arpit *et al.*, “Bolaai: Benchmarking and orchestrating llm-augmented autonomous agents,” *arXiv preprint arXiv:2308.05960*, 2023.

[39] S. Hong, X. Zheng, J. Chen, Y. Cheng, J. Wang, C. Zhang, Z. Wang, S. K. S. Yau, Z. Lin, L. Zhou *et al.*, “Metagpt: Meta programming for multi-agent collaborative framework,” *arXiv preprint arXiv:2308.00352*, 2023.

[40] Y. Chen, J. Arkin, Y. Zhang, N. Roy, and C. Fan, “Scalable multi-robot collaboration with large language models: Centralized or decentralized systems?” *arXiv preprint arXiv:2309.15943*, 2023.

[41] B. Zhang, H. Mao, J. Ruan, Y. Wen, Y. Li, S. Zhang, Z. Xu, D. Li, Z. Li, R. Zhao *et al.*, “Controlling large language model-based agents for large-scale decision-making: An actor-critic approach,” *arXiv preprint arXiv:2311.13884*, 2023.

[42] W. Chen, S. Koenig, and B. Dilkina, “Why solving multi-agent path finding with large language model has not succeeded yet,” *arXiv preprint arXiv:2401.03630*, 2024.

[43] S. S. Kannan, V. L. Venkatesh, and B.-C. Min, “Smart-llm: Smart multi-agent robot task planning using large language models,” *arXiv preprint arXiv:2309.10062*, 2023.

[44] V. Pallagani, K. Roy, B. Muppani, F. Fabiano, A. Loreggia, K. Murgesan, B. Srivastava, F. Rossi, L. Horesh, and A. Sheth, “On the prospects of incorporating large language models (llms) in automated planning and scheduling (aps),” *arXiv preprint arXiv:2401.02500*, 2024.

[45] F. Zeng, W. Gan, Y. Wang, N. Liu, and P. S. Yu, “Large language models for robotics: A survey,” *arXiv preprint arXiv:2311.07226*, 2023.

[46] V. Balasubramanian, S.-S. Ho, and V. Vovk, *Conformal prediction for reliable machine learning: theory, adaptations and applications*. Newnes, 2014.

[47] A. N. Angelopoulos, S. Bates *et al.*, “Conformal prediction: A gentle introduction,” *Foundations and Trends® in Machine Learning*, vol. 16, no. 4, pp. 494–591, 2023.

[48] G. Shafer and V. Vovk, “A tutorial on conformal prediction.” *Journal of Machine Learning Research*, vol. 9, no. 3, 2008.

[49] A. Z. Ren, A. Dixit, A. Bodrova, S. Singh, S. Tu, N. Brown, P. Xu, L. Takayama, F. Xia, J. Varley, Z. Xu, D. Sadigh, A. Zeng, and A. Majumdar, “Robots that ask for help: Uncertainty alignment for large language model planners,” 2023.

[50] B. Kumar, C. Lu, G. Gupta, A. Palepu, D. Bellamy, R. Raskar, and A. Beam, “Conformal prediction with large language models for multi-choice question answering,” *arXiv preprint arXiv:2305.18404*, 2023.

[51] J. Wang, J. Tong, K. Tan, Y. Vorobeychik, and Y. Kantaros, “Conformal temporal logic planning using large language models: Know-

ing when to do what and when to ask for help,” *arXiv preprint arXiv:2309.10092*, 2023.

[52] Y. Xiao and W. Y. Wang, “Quantifying uncertainties in natural language processing tasks,” in *Proceedings of the AAAI conference on artificial intelligence*, vol. 33, no. 01, 2019, pp. 7322–7329.

[53] K. Zhou, D. Jurafsky, and T. Hashimoto, “Navigating the grey area: Expressions of overconfidence and uncertainty in language models,” *arXiv preprint arXiv:2302.13439*, 2023.

[54] Y. Xiao, P. P. Liang, U. Bhatt, W. Neiswanger, R. Salakhutdinov, and L.-P. Morency, “Uncertainty quantification with pre-trained language models: A large-scale empirical analysis,” *arXiv preprint arXiv:2210.04714*, 2022.

[55] A. Angelopoulos, S. Bates, J. Malik, and M. I. Jordan, “Uncertainty sets for image classifiers using conformal prediction,” *arXiv preprint arXiv:2009.14193*, 2020.

[56] H. Yang and M. Pavone, “Object pose estimation with statistical guarantees: Conformal keypoint detection and geometric uncertainty propagation,” in *Proceedings of the IEEE/CVF Conference on Computer Vision and Pattern Recognition*, 2023, pp. 8947–8958.

[57] Z. Mao, C. Sobolewski, and I. Ruchkin, “How safe am i given what i see? calibrated prediction of safety chances for image-controlled autonomy,” *arXiv preprint arXiv:2308.12252*, 2023.

[58] A. Dixit, L. Lindemann, S. X. Wei, M. Cleaveland, G. J. Pappas, and J. W. Burdick, “Adaptive conformal prediction for motion planning among dynamic agents,” in *Learning for Dynamics and Control Conference*. PMLR, 2023, pp. 300–314.

[59] J. Sun, Y. Jiang, J. Qiu, P. T. Nobel, M. Kochenderfer, and M. Schwager, “Conformal prediction for uncertainty-aware planning with diffusion dynamics model,” in *Thirty-seventh Conference on Neural Information Processing Systems*, 2023.

[60] M. Cleaveland, I. Lee, G. J. Pappas, and L. Lindemann, “Conformal prediction regions for time series using linear complementarity programming,” *arXiv preprint arXiv:2304.01075*, 2023.

[61] J. Lekeufack, A. A. Angelopoulos, A. Bajcsy, M. I. Jordan, and J. Malik, “Conformal decision theory: Safe autonomous decisions from imperfect predictions,” *arXiv preprint arXiv:2310.05921*, 2023.

[62] V. Manokhin, “Awesome conformal prediction,” Apr. 2022. [Online]. Available: <https://doi.org/10.5281/zenodo.6467205>

[63] N. Atanasov, J. Le Ny, K. Daniilidis, and G. J. Pappas, “Decentralized active information acquisition: Theory and application to multi-robot slam,” in *2015 IEEE International Conference on Robotics and Automation (ICRA)*. IEEE, 2015, pp. 4775–4782.

[64] A. Singh, A. Krause, C. Guestrin, and W. J. Kaiser, “Efficient informative sensing using multiple robots,” *Journal of Artificial Intelligence Research*, vol. 34, pp. 707–755, 2009.

[65] P. Schillinger, M. Bürger, and D. V. Dimarogonas, “Decomposition of finite ltl specifications for efficient multi-agent planning,” in *Distributed Autonomous Robotic Systems*. Springer, 2018, pp. 253–267.

[66] V. Vovk, “Conditional validity of inductive conformal predictors,” in *Asian conference on machine learning*. PMLR, 2012, pp. 475–490.

[67] M. Sadinle, J. Lei, and L. Wasserman, “Least ambiguous set-valued classifiers with bounded error levels,” *Journal of the American Statistical Association*, vol. 114, no. 525, pp. 223–234, 2019.

[68] E. Kolve, R. Mottaghi, W. Han, E. VanderBilt, L. Weihs, A. Herrasti, M. Deitke, K. Ehsani, D. Gordon, Y. Zhu *et al.*, “Ai2-thor: An interactive 3d environment for visual ai,” *arXiv preprint arXiv:1712.05474*, 2017.

[69] T. Brown, B. Mann, N. Ryder, M. Subbiah, J. D. Kaplan, P. Dhariwal, A. Neelakantan, P. Shyam, G. Sastry, A. Askell *et al.*, “Language models are few-shot learners,” *Advances in neural information processing systems*, vol. 33, pp. 1877–1901, 2020.